Femtosecond Studies of Image-Potential Dynamics in Metals

R. W. Schoenlein and J. G. Fujimoto
Department of Electrical Engineering and Computer Science and Research Laboratory of Electronics, Massachusetts Institute of Technology, Cambridge, Massachusetts 02139

G. L. Eesley and T. W. Capehart
Physics Department, General Motors Research Laboratories, Warren, Michigan 48090
(Received 28 September 1988)

We report the first time-resolved studies of image-potential states on Ag(100). Femtosecond ultraviolet-pump and visible-probe techniques are combined with two-photon photoemission spectroscopy to measure transient photoemission spectra with femtosecond resolution. The lifetime of the $n=1$ image-potential state on Ag(100) is observed to be several tens of femtoseconds.

PACS numbers: 78.47.+p, 73.20.−r, 79.60.Cn

Image-potential states are a unique class of surface states created by the Coulombic attraction between an electron existing outside a material surface, and the electronic image charge in the solid. The electron is essentially trapped between the image potential on the vacuum side and a potential barrier at the crystal surface. This surface barrier is created by a gap of available bulk electronic states in the region about the vacuum potential, and prevents the electron from escaping into the solid. Image-potential states are of particular interest because the wave functions exist primarily outside the material. They form a Rydberg-type series of energy levels with binding energies $E_B \sim 1/n^2$ approaching the vacuum level.[1,2] Higher-order wave functions are localized further in the vacuum; thus the lifetime of the states is expected to increase as n^3.[2] These states provide a unique opportunity for the study of dynamics of a two-dimensional electron gas unaffected by phonon scattering and other processes associated with the crystal lattice.

Shockley[3] first postulated the existence of image-potential states nearly half a century ago, though he did not specify the necessary conditions for bound states. More recently, Echenique and Pendry[2] developed a general theoretical treatment based on wave function phase analysis. Using this approach they predict binding energies for the hydrogenic series, as well as lifetime broadening of the states. Inverse photoemission measurements[4–7] provided the first experimental evidence of image-potential states in metals, and in the past few years high-resolution measurements using two-photon photoemission have identified the $n=1$ and $n=2$ states on surfaces of single-crystal Ag, Cu, and Ni.[8–10] Previously measured linewidths[9] have suggested that these states are long lived relative to bulk states with comparable excess energy; however, measurement accuracy has been limited by instrument resolution and work-function inhomogeneities. Recent developments in the generation and amplification of ultrafast laser pulses now enable direct measurement of excited state lifetimes with femtosecond resolution.

In this paper we present time-resolved studies of image-potential state dynamics on the (100) surface of Ag. By combining optical pump-probe techniques with surface-science techniques we are able to measure transient photoemission energy spectra with temporal resolution on the 10-fs time scale. Photoelectron spectra are generated by use of two-photon photoemission with both visible and ultraviolet femtosecond pulses. An $n=1$ image-potential state lifetime of several tens of femtoseconds is observed. These studies represent the first direct measurement of image-potential state lifetimes and demonstrate that electrons in these states are decoupled from the crystal lattice.

The experiments are performed with a femtosecond laser system consisting of a dispersion-compensated colliding-pulse mode-locked ring dye laser[11] and a copper-vapor laser amplifier[12] operating at 8 kHz. This system produces 55-fs pulses with energies of more than 2 μJ per pulse at a center wavelength of 620 nm (2.00 $\pm$0.02 eV). The amplified pulses are split into pump and probe with the probe delayed relative to the pump by a stepper-motor–driven translation stage. Ultraviolet pulses of $\sim$ 55-fs duration at 4.00 $\pm$ 0.04 eV are generated in the pump arm by frequency doubling of the visible pulses. We use a very thin (100 μm) potassium dihydrogen phosate crystal for second-harmonic generation in order to minimize pulse broadening due to group velocity walk off between the visible and uv pulses. Group-velocity dispersion in the uv resulting from optical elements is compensated by a pair of quartz prisms placed in the pump arm. The visible and uv pulses are combined in a collinear geometry and directed into a vacuum chamber where they are focused onto the sample by a concave mirror.

The experiments are performed on a single-crystal Ag sample cut in a (100) orientation within $\pm 2°$. The sample was polished and placed in a vacuum chamber with a base pressure of 10^{-10} Torr. After repeated cy-

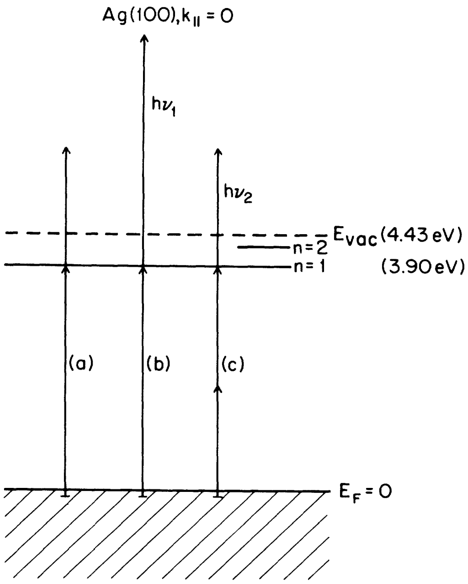

FIG. 1. Energy-level diagram for Ag(100), $k_{\parallel}=0$, showing the various photoemission processes via the $n=1$ state. Lines (a) and (b) represent uv-visible and uv-uv two-photon photoemission; line (c) represents a visible three-photon process.

cles of sputter ion cleaning and annealing, the surface quality was verified using standard LEED and Auger spectroscopy. Photoemitted electrons were detected by a double-pass cylindrical mirror analyzer with an energy resolution of ~ 180 meV at a pass energy of 10 eV.

Figure 1 shows an energy level diagram for the (100) surface of Ag. Near $k_{\parallel}=0$ there is a gap of bulk states centered about the vacuum energy, creating the necessary boundary condition for image-potential states. Previous experimental studies of Ag(100) have measured binding energies of 0.53 and 0.16 ± 0.02 eV for the $n=1$ and $n=2$ states, respectively.[10] Since there are no occupied surface states just below the Fermi energy for the (100) crystal orientation, the $n=1$ image-potential state is populated via nonresonant transitions from occupied bulk states. These transitions involve either one 4.0-eV photon or two 2.0-eV photons, and result in a distribution of excited electrons which extends ~70 meV from the bottom of the $n=1$ band. Electrons are then emitted from the $n=1$ state by either 2.0- or 4.0-eV photons. The $n=2$ state is not populated by these photon energies. Both visible and uv beams were P polarized and no photoemission was observed with S-polarized light, which is consistent with the selection rules for electronic transitions from Δ_1 to Δ_1 states.

Figure 2 shows photoelectron spectra generated by photoemission with uv (left) and visible (right) femtosecond pulses at fluences of ~0.3 and ~0.7 mJ/cm^2, respectively. The maximum photoemission intensity is ~95 counts/s (10^{-2} electron/pulse) for the uv photoemission and ~5 counts/s (10^{-3} electron/pulse) for the visible photoemission. Photoelectron energies are measured relative to the vacuum potential which is determined by the onset of the photoemission signal. In the uv photoelectron spectra we observe a peak at ~3.5 eV corresponding to the $n=1$ image state lying ~0.5 eV below E_{vac}. The relatively large background intensity results from a variety of processes including two-photon photoemission from bulk states and one-photon photoemission enhanced by nonequilibrium electron heating.[13] In addition, because of the acceptance angle of the cylindrical mirror analyzer, the measurement is sensitive to some states extending in the $k_{\parallel}$ direction. The photoelectron yield scales as the square of the incident fluence which is consistent with a two-photon process as well as a thermally-enhanced one-photon process. The peak in the visible (2.0 eV) photoelectron spectra also corresponds to the $n=1$ state. In this case the yield scales as the cube of the incident fluence, consistent with three-photon photoemission. The background intensity is rela-

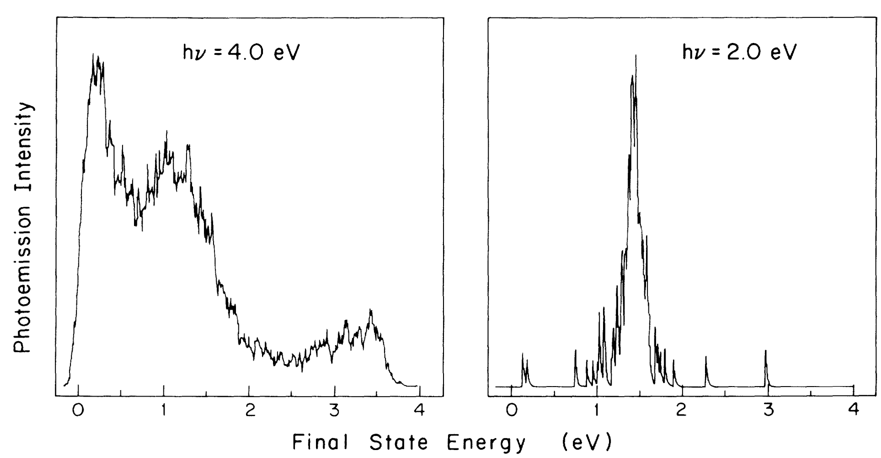

FIG. 2. Photoelectron spectra from Ag(100) with uv pulses (left) and visible pulses (right). Peak photoemission signals are ~10^{-2} electron/pulse and ~10^{-3} electron/pulse, respectively.

tively weak because the 2.0-eV photon energy is insufficient to photoemit from low-energy bulk states.

To study the dynamics of the $n=1$ image-potential state we populate the state with a uv (4.0 eV) pulse and then probe the transient response by photoemitting electrons to the vacuum with a delayed visible (2.0 eV) pulse. This two-wavelength technique is important in time-resolved photoemission because it breaks the symmetry of standard two-photon photoemission, which allows independent control of polarization and a separation of pump effects from those of the probe. The added degree of freedom is instrumental in isolating specific electronic transitions in complicated systems and permits nearly background-free measurements of electron energy spectra on a femtosecond time scale. Furthermore, photoemission from image-potential states with a single 2.0-eV photon is more efficient than photoemission with a uv photon since more than 90% of the uv energy is absorbed via d-band transitions. Thus measurements can be performed at the lowest possible uv fluences, thereby limiting the effects of nonequilibrium electron heating generated by femtosecond pulses,[14] and supressing the two- (4.0 eV) photon background photoemission signal. We do observe evidence of three- (2.0 eV) photon photoemission via the $n=1$ image state; however, the signal is substantially lower than the uv-visible two-photon signal since the process is third order. In all uv-visible measurements the photoemission yield scales linearly with both uv and visible fluences, thus confirming the absence of space-charge effects.

Figure 3 shows a series of two-photon (4.0-eV pump and 2.0-eV probe) photoemission spectra taken at various time delays with positive delay corresponding to visible femtosecond pulses arriving after the uv pulses. The uv and visible fluences are $\sim 6\times 10^{-2}$ and ~ 0.7 mJ/cm^2, respectively, which generate maximum nonequilibrium electron temperatures of a few hundred degrees. This heating has a negligible effect on our image-potential state measurements since the uv pump transitions originate ~ 100 meV below the Fermi level.

The transient photoemission energy spectra show the dynamics of the image-potential state in both energy and time. The rising signal at early times indicates the population of the image state by the femtosecond uv pulse. Spectra at later times show the decay of the excited state within the first 100 fs. The peak appears at ~ 1.5 eV which corresponds to the $n=1$ image-potential state lying ~ 0.5 eV below the vacuum level and is consistent with previously reported results.[10] We measure an energy width of less than 200 meV, which is close to the resolution of our cylindrical mirror analyzer. As expected, the position of this peak remains invariant over the lifetime of the state. Photoemission from the $n=2$ state is not observed since the 4.0-eV pump photon energy is not sufficient to populate this level.

The background photoelectron spectra (inset, $\times 100$ vertical scale) measured at 200-fs delay is shown for reference. We observe a peak at 1.5 eV resulting from three- (2.0 eV) photon photoemission via the $n=1$ image-potential state, and a peak at 3.5 eV corresponds to two- (4.0 eV) photon photoemission from the $n=1$ state. At these time delays we do not detect any photoemission from the combination of uv and visible pulses.

The transient photoelectron spectra indicate an $n=1$ lifetime on the order of the pulse duration. Quantitative results can be obtained through time-resolved measurements of the photoemission at the peak of the energy distribution. Figure 4 shows the dynamics of the $n=1$ state for electrons near the bottom of the image potential band (energy analyzer tuned to 1.5 eV). The solid line is a

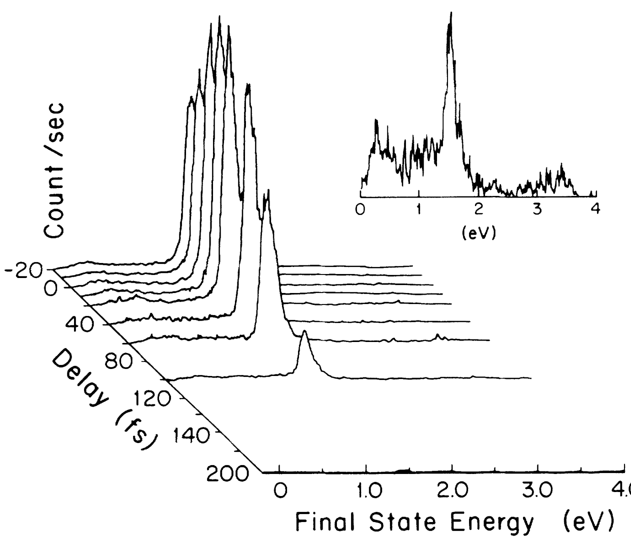

FIG. 3. Photoelectron spectra at various time delays showing the dynamics of the image-potential state. Inset ($\times 100$ vertical scale): the background spectra at +200-fs delay.

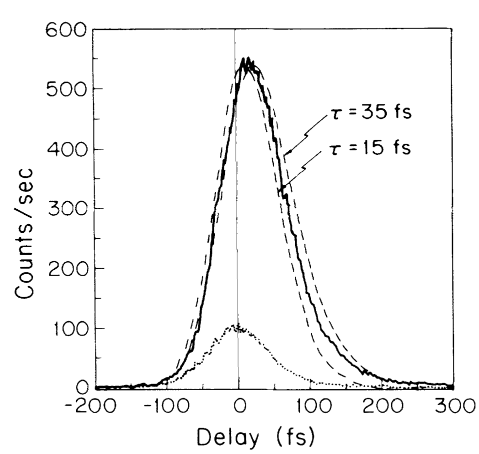

FIG. 4. Lifetime measurements of the $n=1$ image-potential state on a clean Ag(100) surface (solid line) and on an oxygen-dosed surface (dotted line). Dashed lines are convolved exponentials with decay times of 15 and 35 fs.

measure of the image-state lifetime on a clean Ag(100) surface, and the dotted line is a measure of the photoemission from an oxygen-dosed ($\sim 3\times 10^{-4}$ Torr s) surface taken under identical experimental conditions. As expected, the presence of oxygen on the Ag(100) surface quenches the image state lifetime and reduces the photoemission yield. This measurement is used to estimate the uv-visible cross correlation width as well as the zero delay in order to quantify the lifetime of the image-potential state.

The photoemission measurement from the clean surface displays a distinct asymmetry and the peak is shifted toward positive delay (visible following uv) relative to the measurement of the oxygen-dosed surface. This clearly demonstrates the finite duration of the measured lifetime. The asymmetry corresponds to population of the state with uv pulses and photoemission with delayed visible pulses. Because of the finite lifetime, electrons accumulate in the $n=1$ state after the peak of the uv pulse, and thus the maximum photoemission yield occurs after the zero delay. The measurement from the oxygen-dosed surface is quite symmetric, suggesting that the image-state lifetime under these conditions is nearly instantaneous. However, the surface is not saturated with oxygen (as verified by Auger spectroscopy), and measurements of the photoelectron energy distribution width indicate that the lifetime of the $n=1$ state on the oxygen-dosed surface is greater than 4 fs.

We can estimate the lifetime of the $n=1$ image-potential state on the clean surface by assuming a simple exponential relaxation. The photoemission response can then be modeled by convolving the uv-visible cross correlation with a single-sided exponential. The dashed lines show such a convolution using the oxygen-dosed data and exponentials of 15- and 35-fs duration. The accuracy of the fits is limited because the relaxation time is less than the pulse duration, and the uv-visible cross correlation is approximate. Nevertheless, from these results we estimate the $n=1$ image-state lifetime to be in the range of 15–35 fs.

In summary, transient dynamics of the $n=1$ image-potential state in Ag(100) have been investigated with femtosecond ultraviolet-pump and visible-probe techniques combined with two-photon photoemission energy spectroscopy. This novel approach separates the effects of the pump from those of the probe and permits nearly background-free measurements of photoelectron energy spectra with a femtosecond resolution. Our results show the population of the $n=1$ image-potential state and the subsequent relaxation of the electron gas on a time scale comparable to the pulse duration. High-resolution pump-probe measurements at specific photoelectron energies demonstrate an excited state lifetime of several tens of femtoseconds which is within the range predicted by theory.[2,15] Additional studies of higher-order states with a broadband femtosecond uv pump should provide information about the dynamics of these states and their coupling to the crystal lattice. Combining femtosecond pump-probe techniques with angle-resolved photoemission should allow one to investigate the thermalization dynamics of the confined two-dimensional electron gas.

We wish to thank E. P. Ippen for helpful scientific discussions. This research was supported in part by the Air Force Office of Scientific Research under Contract No. F49620-88-C-0089 and the AT&T Foundation. R. W. S. gratefully acknowledges support from the Newport Corporation. J. G. F. gratefully acknowledges support from the National Science Foundation.

[1]M. W. Cole and M. H. Cohen, Phys. Rev. Lett. **23**, 1238 (1969).

[2]P. M. Echenique and J. B. Pendry, J. Phys. C **11**, 2065 (1978).

[3]W. Shockley, Phys. Rev. **56**, 317 (1939).

[4]P. D. Johnson and N. V. Smith, Phys. Rev. B **27**, 2527 (1983).

[5]D. Straub and F. J. Himpsel, Phys. Rev. Lett. **52**, 1922 (1984).

[6]N. Garcia, B. Reihl, K. H. Frank, and A. R. Williams, Phys. Rev. Lett. **54**, 591 (1985).

[7]D. Straub and F. J. Himpsel, Phys. Rev. B **33**, 2256 (1986).

[8]K. Giesen, F. Hage, F. J. Himpsel, H. J. Riess, and W. Steinmann, Phys. Rev. Lett. **55**, 300 (1985).

[9]K. Giesen, F. Hage, F. J. Himpsel, H. J. Riess, and W. Steinmann, Phys. Rev. B **33**, 5241 (1986).

[10]K. Giesen, F. Hage, F. J. Himpsel, H. J. Riess, and W. Steinmann, Phys. Rev. B **35**, 971 (1987).

[11]J. A. Valdmanis, R. L. Fork, and J. P. Gordon, Opt. Lett. **10**, 131 (1985).

[12]W. H. Knox, M. C. Downer, R. L. Fork, and C. V. Shank, Opt. Lett **9** 552 (1984).

[13]J. G. Fujimoto, J. M. Liu, E. P. Ippen, and N. Bloembergen, Phys. Rev. Lett **53**, 1837 (1984).

[14]R. W. Schoenlein, W. Z. Lin, J. G. Fujimoto, and G. L. Eesley, Phys. Rev. Lett. **58**, 1680 (1987).

[15]P. M. Echenique, F. Flores, and F. Sols, Phys. Rev. Lett **55**, 2348 (1985).